17th World Conference on Earthquake Engineering, 17WCEE
Sendai, Japan - September 13th to 18th 2020

SEISMIC EVALUATION OF A BUILDING REPRESENTATIVE OF MASS HOUSING DEVELOPMENT PROJECTS IN CARACAS, VENEZUELA

A. Otero[(1)], C. Molina Hutt[(2)]

[(1)] *Independent Consultant and Researcher*
andresotero@aeoproyectos.com
[(2)] *Assistant Professor, Department of Civil Engineering, University of British Columbia, Vancouver, BC.*
carlos.molinahutt@civil.ubc.ca

Abstract

In an effort to mitigate a considerable housing deficit, the Venezuelan government has constructed many housing development projects using mass production techniques. Most of the developments are in cities with high seismic hazard. The structural system in these buildings consists of reinforced concrete shear walls. They are designed using a linear elastic analysis approach in compliance with the Venezuelan seismic code Covenin 1756, which allows a maximum response modification coefficient (R) as high as 4.5, reducing seismic design forces according to the anticipated ductility of the structural system. The lack of consistency between design assumptions and detailing practices calls the expected performance of these buildings into question. In this study, a 6-story reinforced concrete shear wall building constructed in 2015 is selected to conduct a detailed seismic evaluation in accordance with ASCE 41-13. A numerical 3D model is developed in OpenSees to characterize the nonlinear behavior of the as-built structure. Nonlinear dynamic analyses are carried out to evaluate seismic performance under a suite of ground motions representative of a 475-year return period event. The results suggest the case-study building does not meet the life-safety performance objective inherent in modern building codes. Two major deficiencies are identified: (1) large concentrations of demands in few elements at the base of the structure induce torsional instability; and (2) detailing practices result in limited ductility, suggesting that the design approach should assume considerably lower R values. These preliminary findings highlight the need for further research and a program to review and improve local seismic codes and construction practices in Venezuela.

Keywords: Reinforced Concrete Shear Walls; Seismic Evaluation; ASCE 41; OpenSees; Nonlinear Dynamic Analysis

1. Introduction

Mass housing development projects in Venezuela represent important government investments that have been conceived as a solution to provide thousands of families with suitable homes. Many of the new settlement locations are within seismic-prone regions. The increased exposure, associated with thousands of people relocating to these new sites, results in an amplified seismic risk in these regions. In many of these projects, Reinforced Concrete Shear Walls (RCSWs) are adopted as the main structural system through a process known as *tunnel construction* illustrated in Figure 1a, which is popular due to its speed of construction and reduced costs. There have been no moderate-to-strong earthquakes in Caracas since 1967. The lack of earthquakes prevents a direct evaluation of the seismic performance of this type of construction, or validation of its assumed design parameters.

The ease of use and routine implementation of linear elastic analyses, coupled with inadequate system ductility assumptions through response modification coefficients (R), is generating a false sense of security amongst some structural engineers in Venezuela. The Venezuelan seismic code Covenin 1756 [1] allows R values up to 4.5 for RCSWs systems, but does not limit ductility specifications for thin wall building assemblies, such as those employed in tunnel construction projects. Furthermore, the lack of experimental testing on typical construction sub-assemblies and the paucity in the use of nonlinear dynamic analysis techniques in Venezuela, have resulted in no studies that empirically or analytically validate the many design assumptions in the shear wall system employed in tunnel construction. The goal of this study is to carry out a preliminary seismic performance assessment of an existing 6-story RCSW building erected using the tunnel construction system, which is representative of mass housing construction in Venezuela, as illustrated in Figure 1b. As part of the evaluation, a 3D nonlinear model of the structure is developed in OpenSees [2] and a nonlinear response history analysis (NRHA) is conducted using ground motion records that are representative of the design spectrum prescribed by the Venezuelan seismic specifications.

(a) (b) (c)

Fig. 1 - (a) Tunnel construction in Caracas; (b) Case-study building in Ciudad Caribia Development (6 Ha), conceived to have 37 residential buildings (660 family units) [3]; and (c) Case-study building isometric.

2. Methodology

A seismic evaluation is a process of investigating a building's response and potential deficiencies when subjected to a specified ground motion shaking intensity. The assessment in this study follows of a performance-based approach consistent with a Tier 3 evaluation procedure in ASCE 41 [4], which is applied to the case-study building illustrated in Figure 1c. A life-safety (LS) performance objective is selected, for consistency with the design intent in the Venezuelan code Covenin 1756-1 [1]. This LS objective is associated with a seismic hazard level with a 475-year return period, or 10% probability of exceedance in 50 years, and corresponds to a peak ground acceleration (PGA) of 0.30 g. A 3D model is developed in OpenSees [2], employing multi-layered shell elements capable of explicitly reproducing the expected nonlinear behavior of RCSWs. A suite of ground motions representative of the 475-year hazard level are used to conduct the NRHAs. The performance of the case-study building is evaluated through a series of engineering demand parameters (EDPs) that serve to assess peak median responses against corresponding acceptance criteria. A pushover

analysis is also carried out to estimate global and local ductility demands and evaluate the adequacy of the R factor used in design.

Structural components, namely RCSWs, are classified as either deformation- or force-controlled. Deformation-controlled actions are representative of those with ductile behavior, capable to deform beyond the elastic range without significant loss of strength. Force-controlled actions are representative of brittle components, which result in significant loss of strength beyond the elastic range. The anticipated force versus deformation responses of these components is illustrated in Figure 2a. Primary components are classified as deformation-controlled (consistent with the Type 1 curve in Figure 2a), if the plastic range of response is such that d/g≥2, where d and g denote the plastic limit before lateral strength degradation and the elastic limit, respectively. Otherwise, they are considered as force-controlled (consistent with the Type 3 curve in Figure 2a). Acceptance criteria for deformation-controlled RCSWs elements in nonlinear procedures is determined according to ASCE 41 specifications (Tables 10-19 for components controlled by flexure and 10-20 for components controlled by shear). Acceptance criteria in force-controlled elements is verified by checking that the component's lower-bound strength (Q_{CL}) is not exceeded, in which Q_{CL} is defined as the mean minus one standard deviation of the yield strength (Q_y). The methodology developed for this study is illustrated in Figure 2b and contains the following steps: (1) selection of an existing case-study building and review of construction drawings; (2) performance objective definition based on the design intent of the local seismic code; (3) seismic hazard characterization and selection of hazard consistent ground motions; (4) development of a 3D numerical model with nonlinear attributes capable of capturing expected response that permit checking EDPs against acceptance criteria; (5) processing of nonlinear dynamic analysis results to determine peak median responses and generating a pushover curve to estimate global system ductility; (6) performance assessment of all force-controlled (nonductile) or deformation-controlled (ductile) components against strength or deformation acceptance criteria.

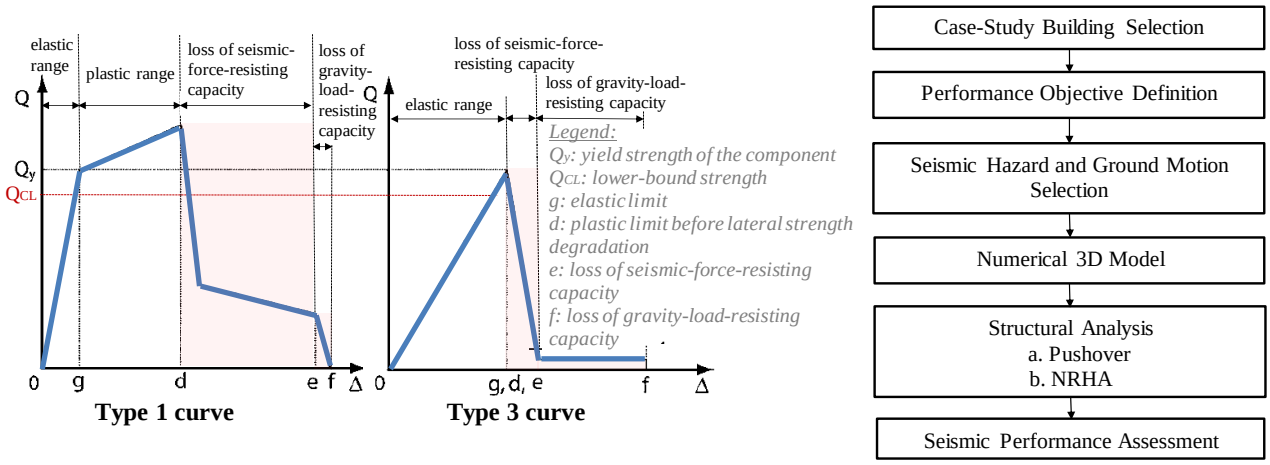

(a) (b)

Fig. 2 - (a) Component force-deformation relations adapted from Fig.7-4 [4]; (b) Assessment methodology.

3. Case-Study Building

The selected building corresponds to a residential mass housing development located in a mountainous region of Venezuela as illustrated in Figure 4a, about 10 Km North West of Caracas. It is a 6-Story building constructed in 2015, which consists of an assembly of shear walls designed to resist both gravitational and lateral loads, and erected with the tunnel construction approach. Per ASCE 7 [5], the building is regular in elevation, but irregular in plan. The seismic weight of the building (~12000 kN) includes self-weight of structural elements (walls and slabs), floor finishes, fixtures and 25% of the live load. Following discussions with local engineers, the design was carried out by means of a modal response spectrum analysis (MRSA) using a response modification coefficient, R, of 4.5, in accordance to the Venezuelan code Covenin 1756 [1], and reinforced concrete specification Fondonorma 1753 [6]. The structural configuration consists of an

orthogonal distribution of RCSWs, with 120 mm to 150 mm in thickness, and slabs of 120 mm in thickness. Concrete compressive strength, f'_c, is 24.5 MPa (3500 psi) and nominal yield strength of steel reinforcement, f_y, is 412 MPa (60 ksi). At the base, the walls include boundary elements, which are detailed with longitudinal reinforcement bars of 13 mm (1/2") in diameter, which are confined with 10 mm (3/8") diameter ties. Longitudinal reinforcement is reduced after the 3rd floor, and the spacing of ties is increased to 0.20 m. All the walls include two layers of welded wire mesh, with a nominal yield strength, f_y, of 490 MPa (70 ksi), to provide minimum reinforcement requirements. The wire mesh grid is 150 mm by 150 mm with a wire diameter of 7 mm. The overall height is 15.20 m above grade with story heights of 2.52 m. Concrete slabs cover a total area of 277.5 m^2 per story and are reinforced with two layers of the same welded wire mesh used in the walls. The building sits above a 300 mm thick concrete mat foundation (24.80 m x 14.90 m). All steel reinforcement is embedded to the bottom face of the foundation. A plan view at the base of the building is ilustrated in Figure 3a, where each wall is asigned a unique identifier and wall assemblies (open wall sections) are identified the the letter W. Elevations along grids C and 4 are illustrated in Figures 3b and 3c, respectively. Typical boundary zone detailing is shown in Figure 3d.

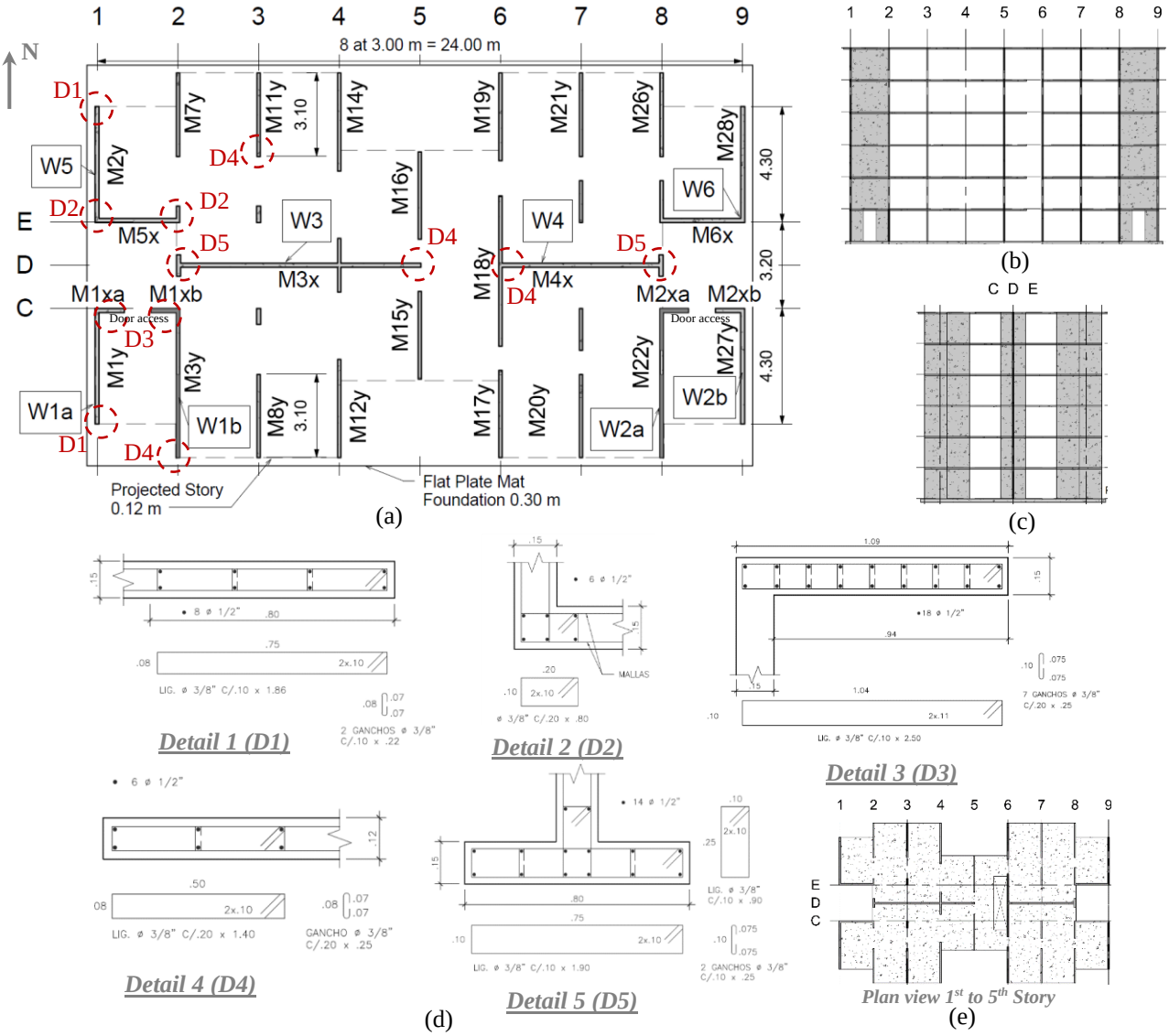

Fig. 3 – (a), (e) Plan views; (b) Elevation Grid C; (c) Elevation Grid 4; and (d) Boundary Element Detailing.

4. Seismic Hazard and Ground Motion Selection

The city of Caracas lies within a complex tectonic plate regime between the boundary of the Caribbean and the South American plate, which strikes east-west at a rate of approximately 20 mm/yr [7], as illustrated in Figure 4a. The case-study building is near known faults, designated by the Venezuelan seismological research center (Funvisis), including San Sebastian and El Avila. These fault structures are key contributors to the seismic hazard of the region, as observed by past earthquake events [8].

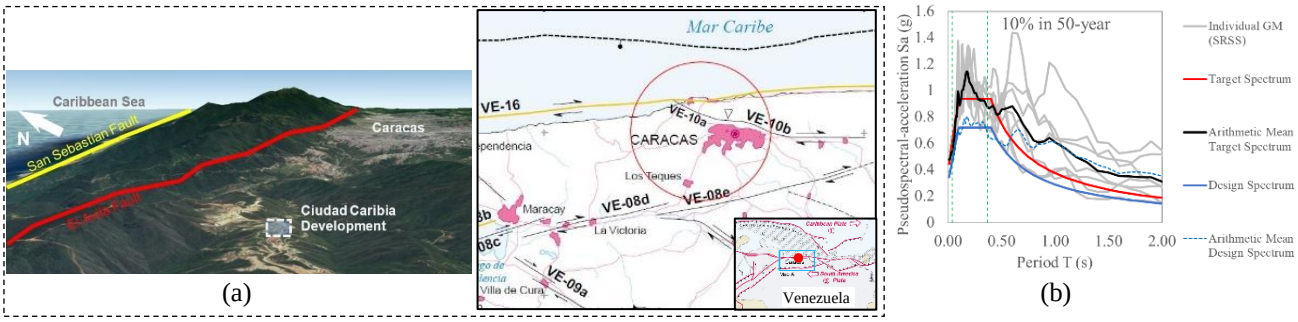

Fig. 4 - (a) Main fault systems contributing to seismic hazard of Caracas, VE-16 (San Sebastian fault) and VE-10a (El Avila fault), sources [9] and [10]; (b) Design spectrum, target spectrum and individual ground motion spectra scaled to match the target in the period range $0.2T_{min}$=0.05 s and $1.5T_{max}$=0.43 s, adapted from [9] and [10].

In order to carry out NRHA of the case-study building, seven ground motion (GM) records are selected from PEER's NGA-West2 [11] database to match the target spectrum. To the extent possible, the records are selected to be hazard consistent (appropriate fault type, magnitude, distance, etc.). The target spectrum is obtained by multiplying the design spectrum by a factor of 1.3 as recommended in the NEHRP [12] guidelines because the intensity measure used to define the design spectrum in Covenin 1756 is the geomean spectral acceleration rather than the maximum direction of response in the horizontal plane. The period range for matching is between $0.2T_{min}$ and $1.5T_{max}$, where T_{max} and T_{min} represent maximum and minimum periods of the building in each principal direction. For the case-study building, the period range of interest lies between 0.04 s and 0.37 s as illustrated in Figure 4b.

5. Numerical Analysis Model

A 3D nonlinear model is developed in OpenSees. The model aims to simulate structural response beyond the elastic limits. A layered shell element, implemented in OpenSees by Lu et al. [13], is selected to reliably simulate the response of RCSWs. As illustrated in Figure 5a, the analytical model was calibrated against experimental test data to ensure the accuracy of the simulation. Component parameters were developed based on member sizes, reinforcement details and strength of materials shown in the construction drawings, discussed earlier in Section 3. Linear properties are assigned to elements where forces are anticipated to be below their yield strength. Gravitational loads are considered by applying a distributed area load to the slabs. Loads (and corresponding seismic mass) include self-weight of structural elements, permanent loads of floors, walls, finishes and a 25% of live load. Seismic masses are lumped at the end and middle nodes along the RCSWs as illustrated in Figure 6b. The walls are assumed to be fixed at the base. Floor diaphragms are explicitly modeled using elastic shell elements. To account for cracking and the nonlinear response of the floor slabs, a reduced moment of inertia of one third is applied to the linear shell elements. A damping ratio of 5% is assumed in the analysis implemented using the Rayleigh damping model. Soil-structure interaction (SSI) is not considered in this assessment. The following paragraphs provide key features of the model, including the shell elements, constitutive concrete, steel material models, and dynamic properties of the case-study building.

Elements. The numerical model is composed by quadrilateral shell elements defined in OpenSees for rectangular shear walls. The ShellDKGQ (1st and 2nd story) is assigned for nonlinear layered sections and the ShellMITC4 (3rd to 6th story) is assigned for elastic sections. Shear walls are planar or combined into "H", "T"

and "C" wall assemblies. The multi-layered shell elements are based on the principles of composite material mechanics by dividing a shear element in several layers as illustrated in Figure 6a, in which each layer is assigned a stress-deformation isotropic or orthotropic parameter and its associated materials constituent laws (e.g. concrete, reinforcing steel, welded wire mesh). It can simulate the in-plane coupled shear/bending behavior and the out-of-plane bending in RCSWs. Truss elements are used to model for longitudinal reinforcing steel as illustrated in Figure 6b. Longitudinal reinforcing steel is connected to shells by sharing the same discretization nodes as the RCSWs.

Concrete Material. Stress-strain uniaxial curves are defined to model concrete within the multilayered shells. The procedure to determine the characteristics of the confined concrete properties within boundary elements (BE) and the wall elements (WE) are based on the methodology specified by Priestley & Paulay [14], which result in the stress-strain curves shown in Figure 5b and corresponding OpenSees parameters seen in Table 1. Aggregate interlock action represented by the Shear Retention Factor (SRF), which represents a reduction of shear stiffness due to cracks, is considered following the recommendations of Ile & Reynouard [15].

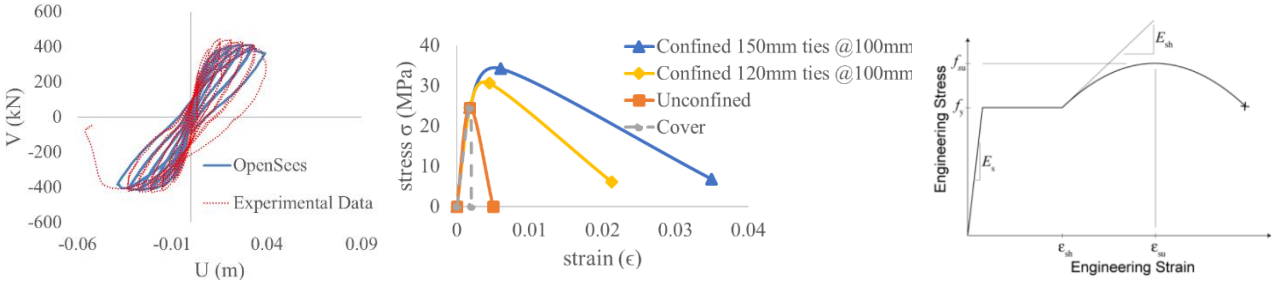

(a) (b) (c)

Fig. 5 – (a) Comparison between OpenSees model and experimental test (data from [13]) and constitutive stress-strain models: (b) concrete and (c) longitudinal reinforcing steel.

Table 1 – OpenSees input for concrete materials.

Type of Element	compressive strength f'_c (MPa)	tensile strength f_t (MPa)	crushing strength f_{cu} (MPa)	strain at max strength ε (-)	strain at crush strength ε_u (-)	strain at max tensile strength ε_{tu} (+)	srf[4]
Boundary Element (BE1)[1]	-34.32	3.07	-6.86	-0.0060	-0.0350	0.0010	0.10
Boundary Element (BE2)[2]	-30.64	3.07	-6.12	-0.0045	-0.0212	0.0010	0.10
Wall Element (WE)[3]	-24.50	3.07	0	-0.0018	-0.0050	0.0010	0.10
Concrete Cover	-24.50	3.07	0	-0.0018	-0.0020	0.0010	0.10

[1] Confined boundary element of t_w=150 mm with 10 mm tie bars @ 100 mm

[2] Confined boundary element of t_w=120 mm with 10 mm tie bars @ 100 mm

[3] Unconfined wall elements between welded wire mesh

[4] Shear retention factor

Steel Material. Two reinforcing steel uniaxial materials are defined, one corresponding to the longitudinal boundary reinforcement as developed by Mohle [16] and illustrated in Figure 5c, and the other to model transverse reinforcement and the welded wire mesh, which follows the Giuffre-Menegotto-Pinto steel material object developed by Filippou [17].

Dynamic Properties. A modal analysis was used to determine the dynamic properties of the building. The first mode is a translational vibration mode in the north-south direction with a period of 0.29 sec. The second mode is a translational vibration mode in the east-west direction with a period of 0.28 sec. The third mode is a torsional vibration mode with a period of 0.27 sec.

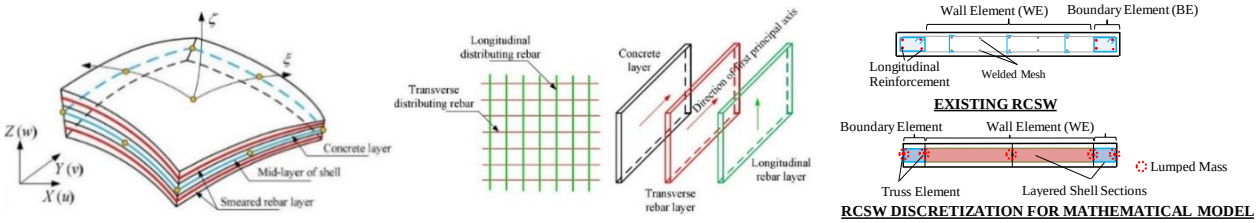

(a) Orientation of "smeared" rebar layers (source: [13]) (b) Truss & mass discretization

Fig. 6 – Multi-layered shell element and RCSW discretization.

6. Results

6.1 Nonlinear Response History Analysis

Time history results for each analysis run, including support reactions, node displacements and element demands, are evaluated to obtain peak EDPs. Median values are then determined from the peak responses of all analysis runs to check against corresponding acceptance criteria. Figure 7 shows median interstory drift ratios measured at the center of mass of each story (each number corresponds to a GM, with IDs consistent to those in the PEER NGA-West2 database). It can be observed that along the east-west direction, drifts are concentrated at the first level, while in the north-south direction there is a more balanced distribution of drifts along the building height. While these drift values are low, tests on lightly reinforced thin walls have illustrated loss of strengths at drifts as low as 0.33% [18]. Torsional effects are measured per ASCE 7 (Table 12.3-1) recommendations. Four nodes are selected to represent the corners of the floor plate at roof level. Along the east west direction, the median (of the seven simulations) ratio between maximum corner displacement and the average displacement is over 1.40, which is consistent with the "Extreme Torsional Irregularity" classification per ASCE 7. Along the north-south direction, values are less than 1.20, which would imply no torsional irregularity.

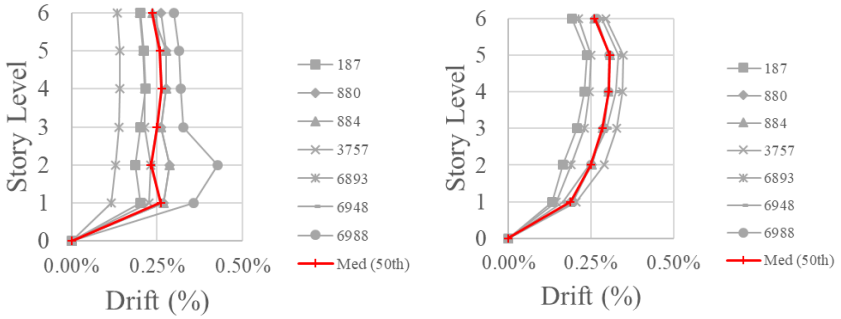

(a) East-West direction (b) North-South direction

Fig. 7- Median drift ratios measured at the center of mass of each level for the seven GMs.

Shear force demands (V_u) are obtained at the base of each wall by adding up horizontal reactions in each restrained node in both orthogonal directions. Shear distortion is also computed for all walls at the first story by evaluating the relative displacements of the corner nodes of each wall panel as illustrated in Figure 8a. Shear nominal capacity (V_n) is determined per equation 18.10.4.1 of the ACI 318 [19]. Figure 8b shows the median shear demand to capacity ratios of all walls at the first story. Along the North-South direction, shear demand is more evenly distributed than along the East-West direction, where most of the shear forces are concentrated in four wall assemblies, with high utilization ratios (near capacity). Force-controlled actions for shear behavior are represented through demand-capacity ratios. Where the shear actions are dominated by inelastic response, drift ratios (Δ/L) outputs are compared against the selected performance level to verify compliance and estimate potential damage. While the results shown median response, in certain wall assemblies in the East-West direction, e.g. M3x, as many as three out of seven simulations result in failure.

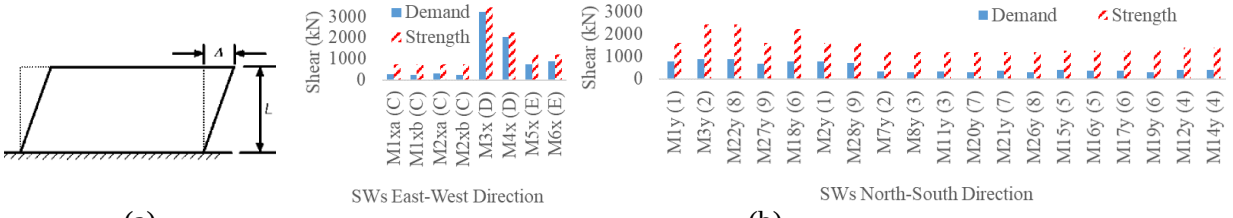

(a) (b)

Fig. 8 – (a) Representation of shear deformation; (b) Shear demand-capacity.

In general, higher axial load stresses and higher shear stresses reduce the ductility of walls. As a result, even flexure-dominated walls can be considered as force-controlled due to their low ductility capacity. Flexural demands are evaluated at the base of each wall in its strong axis. Axial load-bending moment (P-M) interaction diagrams are constructed for each wall using the software CSiCol [20]. For wall assemblies, the direction of loading influences the shape of the P-M interaction diagram. For force-controlled components (flexural behavior), the P_i-M_i time history response at the base of each wall is checked against its corresponding yield moment capacity (M_y) and axial strength (P_n) represented though the P_n-M_y interaction diagram, as illustrated in Figure 9a. For deformation-controlled components where SWs reach the yield surface, plastic hinge rotations θ_i are estimated over the hinge length (l_p), as illustrated in Figure 9b, from the extreme fiber longitudinal strains (ε). Hinge rotations are then checked against corresponding performance objectives, as illustrated in Figure 9c. The yield rotation (θ_y) is estimated following equation 10-5 in ASCE 41.

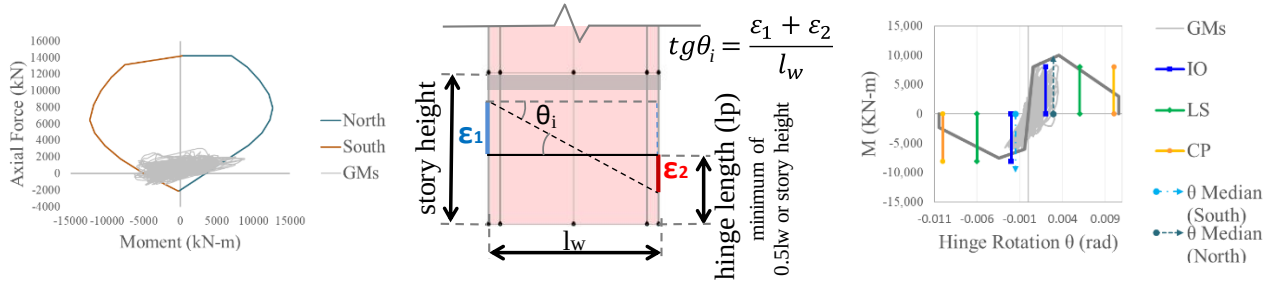

(a) (b) (c)

Fig. 9 – (a) P-M interaction wall M1y; (b) Hinge rotation calculation; (c) M-θ wall M1y.

6.2 Nonlinear Static (Pushover) Analysis

A pushover analysis is performed in each of the building's principal directions to estimate its global ductility and to determine the moment-rotation response of different components. The lateral force pattern is applied based on the fundamental mode shape in the direction under consideration. The node at the center of mass of the roof is set to be the control node. The yield displacement (Δ_y) of the building is determined from the pushover analysis results. Median peak values corresponding to the maximum roof displacement response (Δ_m), as obtained from the NRHA, are then used to determine the displacement ductility ($\mu_\Delta = \Delta_m / \Delta_y$) demands. Ductility demand classification is defined in the ASCE 41 Table 10-6. The displacement ductility is a measure of the energy dissipated [14] and can be related to the seismic force reduction factor R by means of equation 2 [21].

$$R = \sqrt{2\mu - 1} \tag{1}$$

6.3 Performance Assessment

Median peak response values of forces, drifts, moments and rotations derived from the NRHA are determined to assess compliance of each element according to its demand classification. Acceptance criteria for each action is as defined in ASCE 41. Some unsymmetrical wall assemblies have a combination of both deformation and force-controlled actions, which depend on the analysis direction considered. Acceptance criteria for force-controlled components is expressed through demand-capacity ratios (ultimate response/nominal strength). For deformation-controlled components, these are expressed through deformation demands normalized by Life-

Safety deformation limits (inelastic deformation/target performance deformation limit), as defined in ASCE 41 Tables 10-19 (flexure) and 10-20 (shear). Table 2 summarizes the results of the evaluation against governing acceptance criteria. Utilization ratios are also graphically illustrated in Figure 11. It can be appreciated that most of the structural components classify as force-controlled actions with a governing shear behavior in both principal directions. The evaluation suggests that two components (M1xa with a ratio of 1.09 and M2xb with a ratio of 1.02) fail under a force-controlled flexural behavior response, as illustrated in the Figure 10. This type of force-controlled failure is considered brittle and could lead to a partial or global collapse of the building. Both components correspond to a discontinuous SW due to a door access that is used in the base of the building, as displayed in Figure 3b. The configuration generates fluctuating overturning moments imposing large axial forces (tensile and compressive) in each pier. Failure occurs in the east direction for M1ax and the west direction for M2xb, as illustrated in Figure 10. Components centered along grid line D reach high median shear utilization ratios (M3x with a ratio of 0.96 and M4x with a ratio of 0.89) and have significant probabilities of failure, e.g. SW M3x reaches three failure conditions out of the seven simulations.

Along the north-south direction, demands tend to be greater in the perimeter walls, mainly because of larger wall thicknesses, which attract more seismic force, and due to torsional effects combined. Torsional instability could be reached after failure of components M1xa and M2xb due to a shift in the center of stiffness with regards to the center of mass. The highest shear demand in the north-south direction is developed in the assembled wall W5 (M2y with a ratio 0.49). SWs located along grid lines 4, 5 and 6 are the only components governed by a deformation-controlled actions, due to lower values of axial and shear demand, and have low utilization ratios (0.18 in the M12y SW component).

6.5 Ductility

Figure 12 displays the pushover curve and a sample hysteretic response of the control node corresponding to the GM that generates maximum displacements in both directions (GM ID 6988). Along the North-South direction, moderate ductility demands are observed, which can be accommodated by the highly ductile response of all components. In contrast, along the East-West direction, there is a mismatch between the high ductility demands and the limited ductility of some of the walls. Evaluating peak deformation demands in relation to yield deformations, serves to estimate the ductility capacity of the system in each direction and the associated response modification factor, R. These parameters, illustrated in Table 3, suggest that the R factors assumed in the code drastically overestimate the ductility of the system in the East-West direction.

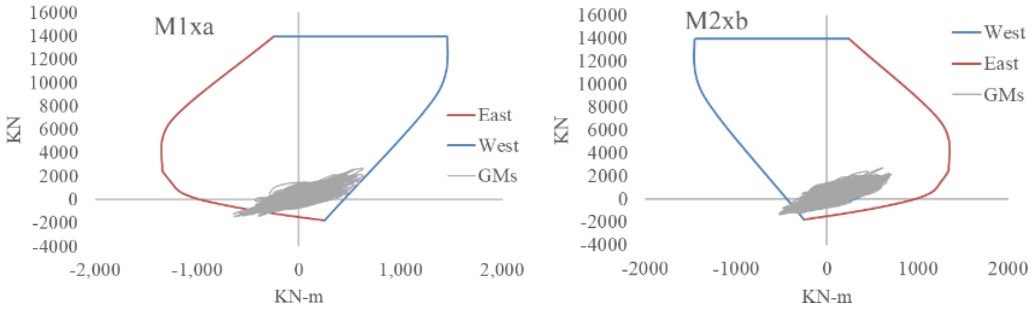

(a) M1xa (b) M1xb

Fig. 10 - Interaction curves with P-M time history response for flexural force-controlled behavior.

Table 2 – Evaluation results.

Characteristics[1]						Shear Behavior										Flexural Behavior[12]						
SW Name (Grid)	Dir	t_w (mm)	l_w (mm)	A_s (mm^2)	A_s' (mm^2)	N_u[2] max. (kN)	Axial[3] Cond. eq.	Shear[4] Parameters d(%)	Shear[4] Parameters g(%)	d/g[5]	Dem.[6] Act. Class.	V_u(kN)[7] or Δ_i/L_i (%)	V_n (kN)[8] or LS (%)	D/C[9]	Dem.[10][5] Act. Class.	Shear[11] Cond. eq.	Elastic rot. limit (rad)	Total rotation (rad)	Plastic rotation (rad)	M_n (kN-m)[13] or LS (rad)	D/C[9]
In-plane Shear Response (North-South) at base level																						
W1a	N	150	4300	1032	2322	2206	0.07	0.8	0.4	1.88	**F-C**	771	1625	**0.47**	D-C	6.2	0.0004	0.0029	0.0025	0.006	0.41
M1y (1)	S			2322	1032		0.12	0.8	0.4	1.88							0.0006	0.0015	0.0009		0.15
W1b	N	120	5550	516	2322	1591	0.03	1	0.4	2.50	D-C	0.10%	1.5%	0.07	D-C	7.0	0.0005	0.0020	0.0015	0.006	0.25
M3y (2)	S			2322	516		0.10	0.8	0.4	1.88	**F-C**	897	2427	**0.37**			0.0007	0.0011	0.0005		0.08
W2a	N	120	5550	516	2322	2131	0.05	1	0.4	2.50	D-C	0.11%	1.5%	0.08	D-C	6.8	0.0005	0.0023	0.0017	0.006	0.29
M22y (8)	S			2322	516		0.12	0.8	0.4	1.88	**F-C**	874	2427	**0.36**			0.0007	0.0013	0.0006		0.10
W2b	N	150	4300	1032	2322	2445	0.08	0.8	0.4	1.88	**F-C**	694	1625	**0.43**	D-C	5.6	0.0002	0.0009	0.0007	0.006	0.12
M27y (9)	S			2322	1032		0.13	0.8	0.4	1.88							0.0005	0.0009	0.0004		0.06
W4	N	120	5600	774	774	3432	0.14	0.8	0.4	1.88	**F-C**	782	2241	**0.35**	D-C	6.1	0.0011	0.0010	-	0.006	elas.
M18y (6)	S			774	774		0.14	0.8	0.4	1.88								0.0009	-		elas.
W5	N	150	4300	774	1032	1329	0.05	0.8	0.4	1.88	**F-C**	800	1625	**0.49**	D-C	6.5	0.0004	0.0019	0.0015	0.006	0.24
M2y (1)	S			1032	774		0.06	0.8	0.4	1.88							0.0002	0.0025	0.0023		0.39
W6	N	150	4300	774	1032	1447	0.06	0.8	0.4	1.88	**F-C**	720	1625	**0.44**	D-C	5.8	0.0004	0.002	0.0013	0.006	0.21
M28y (9)	S			1032	774		0.07	0.8	0.4	1.88							0.0002	0.002	0.0019		0.31
Rectangular SWs (tw=120 mm; lw=3100 mm) - (North-South) at base level																						
M7y (2)						697	0.05	0.8	0.4	1.88	**F-C**	348	1192	**0.29**	D-C	4.88		0.0017	0.0014	0.008	0.18
M8y (3)						1074	0.08	0.8	0.4	1.88	**F-C**	294	1192	**0.25**	D-C	4.12		0.0015	0.0012	0.008	0.15
M11y (3)				507	507	1024	0.07	0.8	0.4	1.88	**F-C**	340	1192	**0.29**	D-C	4.77	0.00027	0.0014	0.0011	0.007	0.17
M20y (7)						1153	0.08	0.8	0.4	1.88	**F-C**	316	1192	**0.27**	D-C	4.43		0.0012	0.0009	0.008	0.12
M21y (7)						1183	0.09	0.8	0.4	1.88	**F-C**	374	1192	**0.31**	D-C	5.24		0.0012	0.0009	0.008	0.11
M26y (8)						719	0.05	0.8	0.4	1.88	**F-C**	320	1192	**0.27**	D-C	4.49		0.0013	0.0010	0.008	0.12
Rectangular SWs (tw=120 mm; lw=3250 mm) - (North-South) at base level																						
M15y (5)						539	0.04	1	0.4	2.50	**D-C**	0.17%	1.5%	**0.11**	D-C	5.35		0.0015	-		elas.
M16y (5)				507	507	551	0.04	1	0.4	2.50	**D-C**	0.17%	1.5%	**0.11**	D-C	5.16	0.00028	0.0015	-	0.008	elas.
M17y (6)						754	0.06	0.8	0.4	1.88	**F-C**	360	1255	**0.29**	D-C	4.81		0.0010	0.0007		0.09
M19y (6)						676	0.05	1	0.4	2.50	**D-C**	0.14%	1.5%	**0.09**	D-C	4.24		0.0010	0.0007		0.09
Rectangular SWs (tw=120 mm; lw=3650 mm) - (North-South) at base level																						
M12y (4)				507	507	497	0.04	1	0.4	2.50	D-C	0.14%	1.5%	0.09	**D-C**	4.88	0.00032	0.0016	0.0013	0.007	**0.18**
M14y (4)						502	0.04	1	0.4	2.50	D-C	0.14%	1.5%	0.09	**D-C**	4.71		0.0014	0.0011	0.007	**0.16**
In-plane Shear Response (East-West) at base level																						
W1a	E	150	1060	580	1741	2166	0.27	0.8	0.4	1.88	F-C	279	754	0.37	**F-C**	9.1	-	-	437	400	**1.09**
M1xa (C)	W			1741	580		0.47	0.8	0.4	1.88					D-C		0.0010	0.0016	0.0006	0.002	0.30
W1b	E	150	1060	1741	580	1127	0.29	0.8	0.4	1.88	F-C	253	754	0.34	D-C	8.3	0.0010	0.0015	0.0005	0.002	0.24
M1xb (C)	W			580	1741		0.09	0.8	0.4	1.88					**F-C**		-	-	241	480	**0.50**
W2a	E	150	1060	580	1741	1052	0.08	0.8	0.4	1.88	F-C	304	754	0.40	**F-C**	10.0	-	-	379	500	**0.76**
M2xa (C)	W			1741	580		0.28	0.8	0.4	1.88					D-C		0.0010	0.0014	0.0003	0.002	0.17
W2b	E	150	1060	1741	580	2126	0.47	0.8	0.4	1.88	F-C	249	754	0.33	D-C	8.2	0.0010	0.0010	-	0.002	elas.
M2xb (C)	W			580	1741		0.26	0.8	0.4	1.88					**F-C**		-	-	357	350	**1.02**
W3	E	150	9100	1806	516	2044	0.05	0.8	0.4	1.88	**F-C**	3309	3440	**0.96**	D-C	12.6	0.0011	0.0015	0.0004	0.006	0.06
M3x (D)	W			516	1806		0.03	1	0.4	2.50	D-C	0.24	1.5	0.16	D-C		0.0009	0.0012	0.0003		0.05
W4	E	150	6120	1032	1806	1768	0.04	1	0.4	2.50	D-C	0.23%	1.5%	0.15	D-C	11.5	0.0013	0.0016	0.0003	0.006	0.05
M4x (D)	W			1806	1032		0.06	0.8	0.4	1.88	**F-C**	2020	2267	**0.89**			0.0010	0.0013	0.0003		0.04
W5	E	150	3150	774	774	1275	0.07	0.8	0.4	1.88	**F-C**	732	1190	**0.62**	D-C	8.1	0.0004	0.0017	0.0013	0.006	0.22
M5x (E)	W			774	774		0.07	0.8	0.4	1.88					D-C		0.0002	0.0016	0.0014		0.23
W6	E	150	3150	774	774	1610	0.09	0.8	0.4	1.88	**F-C**	878	1191	**0.74**	D-C	9.7	0.0005	0.0013	0.0008	0.006	0.14
M6x (E)	W			774	774		0.09	0.8	0.4	1.88					D-C		0.0007	0.0014	0.0007		0.12

[1] Dir: analysis direction considered; t_w: SW thikness; l_w: SW length; A_s: Area of reinforcement in tension; A_s': Area of reinforcement in compression; see Fig. 3a for component name

[2] Peak median axial force of the seven simuations

[3] Axial condition equation specified in tables 10-19 and 10-20 of ASCE 41 to determine modeling parameters and numerical acceptance criteria

[4] Force-deformation relation for shear behavior is assumed to develop a triliniar response as Fig. 10-1c of the ASCE 41; d and g parameters are obtained from Table 10-20 ASCE 41

[5] d: plastic limit before lateral strength degradation; g: elastic limit (Figure 2a); d/g≥2 component is deformation-controlled; d/g≤2 component is Force-Controlled

[6] Demand action classification: Force-Controlled (F-C) or Deformation-Controlled (D-C). Bold represents the governing behavior

[7] Median peak shear demand (kN); or median peak shear drift distortion (%)

[8] Lower-bound shear strength V_n (kN); or LS limit state (rad) from Table 10-20 ASCE 41

[9] Demand capacity ratio >1 implies a non-compliance condition; force-controlled (ultimate response/nominal strength); deformation-controlled (inelastic deformation/target performance)

[10] Force-deformation relation for flexural behavior is obtained from the pushover analysis which generated type curves 1 (Fig. 2a) for each component where relation d/g is assessed

[11] Shear condition equation specified in table 10-19, ASCE 41 to determine modeling parameters and numerical acceptance criteria

[12] Yield rotation point θ_y; Peak median rotation θu; Plastic rotation θ_u-θ_y

[13] Moment lower-bound strength M_n (kN-m) at yield surface coupled with peak M_i-P_i reached at the base of the wall; or LS limit state (rad) from Table 10-19 ASCE 41

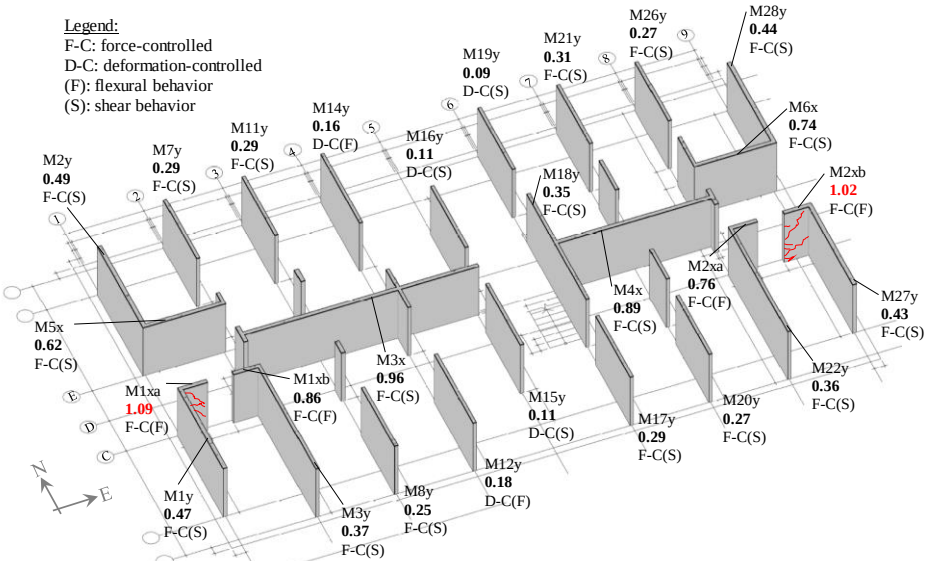

Fig. 11 – Schematic isometric representation (1st level) of acceptance criteria utilization ratios.

Table 3 – Ductility demands.

	East	West	North	South
Global Elastic Limit (Pushover)				
Δ_y (m)	0.0062		0.012	
Median maximum response				
Δ_m [1] (m) (Global)	0.035	0.030	0.035	0.039
Δ_{mf} [2] (m) (Local)	0.009	0.010	0.40	0.21
Displacement Ductility Demand [3]				
$\mu_\Delta=\Delta_m/\Delta_y$ (Global)	5.7	4.9	2.9	3.3
Ductility demand [4]	High		Moderate	
$\mu_\Delta=\Delta_{mf}/\Delta_y$ (Local)	1.5	1.6	33.3	17.5
Ductility Capacity [5]	Low		High	
Response Modification Coefficient [6] (R)				
Local	1.4	1.5	8.1	5.8

[1] Median peak displacement at Roof obtained from the NRHAs

[2] Median peak displacement at roof when the 1st failure is reached at component M1xa

[3] See component ductility demand classification in Table 10-6, ASCE 41

[4] Required ductility demand based on median peak response

[5] Ductility demand capacity based on 1st local failure

[6] Response modification coefficient R coupled with the displacement ductility demand at 1st local failure, see equation (1)

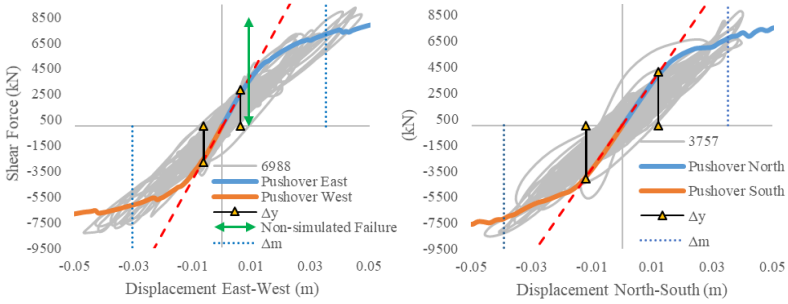

Fig. 12 – Pushover curves.

7. Conclusions and Recommendations

It was found that the case-study building does not comply the seismic performance objective intended by the Venezuelan seismic code Covenin 1756 [2]. Results suggest the case study building has a low ductility in the east-west direction coupled with concentrated seismic demands at the base of the building in few components and low utilizations in other elements. The flexural strength of two force-controlled components is in the E-W direction is exceeded, suggesting these localized brittle failures could lead to partial or total collapse of the building. The results of the study suggest that that a response modification coefficient R should not be higher than 1.4 along the east-west direction, while the assumed 4.5 in design is adequate along the north-south direction. The study also identifies the torsional sensitivity of the design, which would fall under the "Extreme Torsional Irregularity" classification per ASCE 7. While this study is limited to a case study building, it is representative of mass housing development projects in Venezuela. Further research is needed to identify whether similar observations apply more broadly to this type of *tunnel construction* with widespread use.

8. References

[1] Covenin 1756-1, *Edificaciones Sismorresistentes Parte 1: Requisitos,* Caracas: Fondonorma, 2001.

[2] F. McKenna, S. Mazzoni y G. Fenves, *Open System for Earthquake Engineering Simulation,* Berkeley: University of California, 2004.

[3] E. Montilva, *La ciudad utópica del socialismo,* Madrid: El País, 2013.

[4] ASCE 41-13, *Seismic Evaluation and Retrofit of Existing Buildings,* Reston, Virginia: American Society of Civil Engineers, 2013.

[5] ASCE 7, *Minimum Design Loads for Building and Other Structures,* Reston, Virginia: American Society of Civil Engineers, 2010.

[6] Fondonorma 1753, *Proyecto y Construcci'on de Obras en Concreto Estructural,* Caracas: Fondonorma, 2006.

[7] USGS, «Earthquake Hazards,» 2019. [En línea]. Available: https://www.usgs.gov/natural-hazards/earthquake-hazards. [Último acceso: May 2016].

[8] J. Grases y M. Lugo, Catálogo de Sismos Sentidos o Destructures: Venezuela 1530 - 1998, Caracas: Editorial innovación técnica, 1997.

[9] Google Earth, «Ciudad Caribia, Caracas Venezuela. 10° 32’ 10”N, 67° 02’ 09”W, Eye alt 1251 m.,» 2006. [En línea]. Available: https://earth.google.com. [Último acceso: 5 May 2017].

[10] Funvisis, *Venezuelan Seismic Hazard Maps,* Fundación Venezolana de Investigaciones Sismológicas, 2017.

[11] T. D. Ancheta, R. B. Darragh, J. P. Stewart, E. Seyhan, W. J. Silva, B. S.-J. Chiou, K. E. Wooddwell, R. W. Graves, A. R. Kottke, D. M. Boore, T. Kishida y J. L. Donahue, «PEER Ground Motion Database,» 2014. [En línea]. Available: https://ngawest2.berkeley.edu/. [Último acceso: 2016].

[12] NEHRP Consultants Joint Venture, *NIST 11-917-15 Selecting and Scaling Earthquake Ground Motions for Performing Response-History Analyses,* Gaithersburg, Maryland: National Institute of Standards and Technology, 2011.

[13] X. Lu, L. Xie, X. Lu y Y. Huang, «Multi-Layer Shell Element for Shear Walls in OpenSees,» June 2014. [En línea]. Available: https://www.researchgate.net/publication/269192656.

[14] M. J. N. Priestley y T. Paulay, Seismic Design of Reinforced Concrete and Masonry Buildings, First ed., New York, New York: Wailey Interscience Publication, 1992.

[15] N. Ile y J. Reynouard†, «Nonlinear Analysis of Reinforced Concrete Shear Wall Under Earthquake Loading,» vol. 4:2, pp. 183-213, 2006.

[16] J. Mohle, *Reinforcing Steel Material.*

[17] F. Filippou, «Steel02 Material Giuffré-Menegotto-Pinto Model with Isotropic Strain Hardening,» 2006. [En línea]. Available: https://opensees.berkeley.edu/wiki/index.php/UniaxialMaterial_Command. [Último acceso: 2015].

[18] H. Layssi, W. D. Cook y D. Mitchell, *Seismic Response and CFRP Retrofit of Poorly Detailed Shear Walls,* vol. 16.3, Journal of Composites Construction, 2012, pp. 332-339.

[19] ACI-318, *Building Code Requirements for Structural Concrete and Commentary,* Farmington Hills, MI: American Concrete Institute, 2014.

[20] I. Computers and Structures, *CSiCol Design of Simple and Complex Reinforced Concrete Columns,* Berkeley, California, 1975.

[21] A. Chopra, Dynamics of Structures, 3rd Edition ed., Upper Saddle River, New Jersey: Pearson Prentice Hall, 2007.

